Turk J Phys
28 (2004) , 309 – 323.

Thermochemical and Green Luminescence Analysis of Zinc Oxide Thin Films Grown on Sapphire by Chemical Vapor Deposition

Abdelkader DJELLOUL[1], **Rabadan Abdulkadirovich RABADANOV**[2]
[1] *Laboratoire des Matériaux, Structure des Systèmes Electroniques et leur Fiabilité, Centre Universitaire d'Oum El Bouaghi, ALGÉRIE*
[2] *Department of the Physical Electronics, Daghestan State University, RUSSIA*

Received 21.07.2003

Abstract

This study has been carried out to detail an integral thermochemical analysis of the principal reaction in the production of zinc oxide (ZnO) thin films, including developing an analytical form of the equilibrium constant. Zinc oxide thin films prepared by chemical vapor deposition have been studied in terms of deposition time and substrate temperature. The growth of the single-crystal films present two regimes depending on the substrate temperature, with increasing constant growth rates at lower, and higher, temperature ranges, respectively. Growth rates above 6 μm$\cdot$min^{-1} can be achieved at $T_s = 880$ K. The variation of the green luminescence intensities in ZnO single-crystal thin films according to the subsequent processing in hydrogen atmosphere have been studied. After annealing of each ZnO sample at different temperatures, the luminescence intensity is maximal for $\lambda = 510$ nm. It is established that the concentration of the oxygen vacancies could be controlled to within two orders of magnitude for temperatures less than 980 K. Beyond 980 K, defects of interstitial zinc is created in the ZnO films.

Key Words: Zinc oxide, chemical vapor deposition, thermochemical, activation energy, hydrogen annealing, green emission.

1. Introduction

Zinc oxide (ZnO) is a wide-band-gap semiconductor (3.3 eV) with potential for applications as emitter devices in blue to ultraviolet region and as a substrate material for GaN based devices. Pure and doped ZnO thin films have been the subject of much investigation in the past because the ZnO system has many important technological applications, such as in luminescent materials [1] or in piezoelectric devices, of which it has a reasonably large piezoelectric coefficient. Acoustoelectrical devices, such as surface acoustic wave devices (SAW), have been fabricated with ZnO [2, 3]. Due to its unique conducting mechanism based on oxygen vacancies, zinc oxide is also used in oxygen gas sensors [4]. Optical UV lasing has already been observed at room temperature [5]. A variety of methods have been reported for the preparation of ZnO thin films. For example, films have been deposited by thermal evaporation [6], RF sputtering [7, 8], spray pyrolysis [9] laser ablation [10], and variations on these methods [11–14]. In addition to these techniques, chemical vapor deposition method has been widely used process for growing ZnO thin films owing to its excellent versatility and suitability for mass production [15].

For the application of ZnO in electronic materials, the control of intrinsic defects is essential since the electrical properties are largely affected not only by extrinsic dopants but also by intrinsic defects. The atomic and electronic structure of the intrinsic defects in ZnO has been extensively investigated by a variety of experimental methods, e.g., electron paramagnetic resonance (EPR) [16–19], cathodoluminescence [20, 21], deep-level transient spectroscopy [22, 23], positron annihilation spectroscopy [20, 24–26], and perturbed angular correlation spectroscopy [27, 28]. Photoluminescence (PL) properties of the zinc oxide, as well as the electrical properties, depend directly on the growth conditions of ZnO thin films, and on their subsequent processing. The method for ZnO films elaboration is characterized by the intensity of the luminescent band with maximum wavelengths in the range from 500 nm to 530 nm. Several works [29–31] have studied this band and the luminescent yellow-orange band ($\lambda_{\max}$ = 590–620 nm). Various mechanisms have been proposed to explain the ZnO green luminescence. Many authors explored the green luminescence mechanism of ZnO by combining PL, optical absorption and EPR spectrum. Their results showed that the green luminescence is induced by the singly ionized oxygen vacancies in the form of F^+ centers [30, 32]. The study of the EPR spectrum of F^+ centers in the ZnO single-crystal indicates that the oxygen vacancy V_O in the system can be neutral, and represents a deep donor with the ionization energy equal to 2.7 eV [33]. Such centers are not responsible for the high electrical conductivity of ZnO, but are entirely able to radiate the light at λ = 510 nm [34]. Despite this, there are many contradictory and litigious questions concerning the interpretation of these bands. Recent electron paramagnetic resonance measurements of commercial ZnO powders and powders prepared by SP (spray pyrolysis) at 973–1173 K show the relationship between singly ionized oxygen vacancies and the green luminescence [35, 36]. These vacancies grow rarer while penetrating deeply the crystallites [9].

In our opinion, the most important studies involve samples obtained in controlled conditions, and exposed to appropriate processing. The aim of this work has been to obtain ZnO single crystal thin films by chemical vapor deposition under controlled conditions. In section 2 we present the integral thermochemical analysis of the principal reaction to obtain zinc oxide thin films and growth conditions. In section 3, we investigate (a) the green luminescence of ZnO thin films and (b) the nature of the variation of the green luminescence intensities according to the conditions of the subsequent processing in a hydrogen atmosphere.

2. Experiment

The chemical vapor deposition (CVD) method has been widely used process for growing ZnO thin films owing to its excellent versatility and suitability for mass production. Another advantage of the chemical vapor deposition technique is that it can be adapted easily for production of single-crystal thin film thickness $\sim$2 mm. The ZnO films were prepared in a vertical hot-wall CVD type reactor, illustrated in Figure 1. The CVD apparatus consists of: (1) electric furnace, (2) quartz tube reactor, (3) substrate holder (4) crucible, (5) substrate, (6) thermocouple, (7) reactor holder, (8) cover, (9) guard heater, (10) pressure sensor and (11) to vacuum pump. The films were prepared on sapphire (Al_2O_3) substrates under H_2 atmosphere. The total pressure P_{tot} was controlled from 0.117 to 0.216 MPa and the deposition temperature T_{crucible} was varied from 900 K to 1100 K. The substrate temperatures used in our experiment ranged from 800 K to 960 K. The samples studied were grown under the reaction

$$\mathrm{ZnO_{(c)}} + \mathrm{H_{2(g)}} \rightleftarrows \mathrm{Zn_{(g)}} + \mathrm{H_2O_{(g)}}. \tag{1}$$

where The hydrogen (H_2) was used as the carrier gas to transport the reactant.

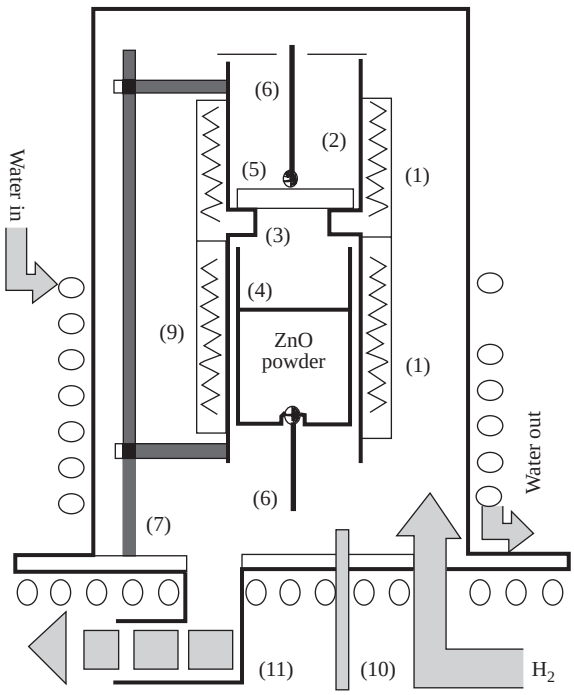

Figure 1. Schematic diagram of the vertical hot-wall CVD apparatus.

Of ZnO films that are obtained by reaction (1), the luminescence intensity is maximal for $\lambda_{\max} = 510$ nm, not only in the as-cast condition but also after being heat-treated in air.

After deposit the samples are annealed in a furnace using a quartz tube reactor. Photoluminescence (PL) spectra were measured at room temperature using a home-assembled system. PL spectra were measured using a Bentham TM300 multiple grating monochromator. The PL was excited by a Xe arc lamp with output at wavelength 415 nm. The samples were formed of ZnO single crystal thin films (thickness $\sim$2 mm) grown on sapphire (Al_2O_3) at $T_{\text{crucible}} = 990$ K and $T_{\text{substrate}} = 880$ K.

3. Results and Discussions

3.1. Thermochemical study of reaction (1)

The specific relation between such reaction and growth conditions is not clear unclear. Because of its high vapor pressure, growth of ZnO from melt is difficult, and similarly growth by vapor deposition is difficult to control. In order to understand ZnO growth mechanisms from the gas phase, it is important to clarify the specific relation by a thermochemical study of reaction (1).

A description of such a chemical vapor disposition process must therefore contain four elements: (1) mass transport to substrate, (2) incorporation of individual species on to the substrate by thermally activated kinetic processes, (3) mass transport along the substrate surface by surface diffusion, and (4) re-evaporation of the absorbed species into the gas phase.

The possibility of a reaction (1) taking place is governed by:

1 (a) the change in enthalpy ΔH accompanying the reaction,
(b) the change in entropy ΔS of the system,
and the combined effects of these two factors is shown in terms of free energy (ΔG) change;
2 the mechanism of the reaction and the speed with which it takes place.

The heat change accompanying a chemical reaction depends only on the final and initial states of the system, and is independent of all intermediate states (Hess's law). This means that it is possible to determine

the heat change for a reaction (1) which does not take place directly, by summing up a succession of the intermediate reactions as:

$$\left.\begin{array}{c} \mathrm{ZnO_{(c)}} \rightleftarrows \mathrm{Zn_{(c)}} + \frac{1}{2}\mathrm{O_{2(g)}} \\ \mathrm{Zn_{(c)}} \rightleftarrows \mathrm{Zn_{(l)}} \\ \mathrm{Zn_{(l)}} \rightleftarrows \mathrm{Zn_{(g)}} \\ \mathrm{H_{2(g)}} + \frac{1}{2}\mathrm{O_{2(g)}} \rightleftarrows \mathrm{H_2O_{(l)}} \\ \mathrm{H_2O_{(l)}} \rightleftarrows \mathrm{H_2O_{(g)}} \end{array}\right\}. \tag{2}$$

The symbols (g), (l) and (c), indicate whether the substance taking part in the reaction is gas, liquid or crystalline solid, respectively.

The rate of change of the heat of reaction ΔH with the temperature in terms of the heat capacities of the substances involved is given by the Kirchhoff equation as

$$\left(\frac{\partial\left(\Delta H\right)}{\partial T}\right)_P = \Delta C_p = \sum\left(\Delta C_p\right)_{\text{products}} - \sum\left(\Delta C_p\right)_{\text{reactants}}. \tag{3}$$

The standard heat of formation, the heat of the phase transformations, and the heat capacities with respect to the temperature of the components taking part in reaction (2), are presented in Table 1, [37, 38, 39].

Table 1. Thermodynamic properties of same compounds interest.

Species	Enthalpy $\Delta H^0_{f(298.15)}$	Entropy $S^0_{298.15}$	$H_{l\rightleftarrows c}$	$H_{g\rightleftarrows l}$
	$J{\cdot}mol^{-1}$	$J{\cdot}mol^{-1}{\cdot}K^{-1}$	$J{\cdot}mol^{-1}$	$J{\cdot}mol^{-1}$
ZnO	-348110	43.7		
Zn		41.69	7403.7 (692.7 K)	115476 (1180 K)
H_2		130.8		
O_2		205.32		
H_2O	-285830	70.18		40936.3

Species	Heat capacity $C_{p(c)}$	Heat capacity $C_{p(l)}$	Heat capacity $C_{p(g)}$
	$J{\cdot}mol^{-1}{\cdot}K^{-1}$	$J{\cdot}mol^{-1}{\cdot}K^{-1}$	$J{\cdot}mol^{-1}.K^{-1}$
ZnO	$49.06 + 5.11\times10^{-3}T - 9.13\times10^{5}T^{-2}$ (273–1573 K)		
Zn	$22.42 + 10.50\times10^{-3}T$ (273–692.7 K)	31.42	20.82
H_2			$27.32 + 3.27\times10^{-3}T + 0.50\times10^{5}T^{-2}$ (273–2500 K)
O_2			$31.51 + 3.39\times10^{-3}T - 3.77\times10^{5}T^{-2}$ (300–5000 K)
H_2O		75.54	$30.04 + 10.73\times10^{-3}T + 0.33\times10^{5}T^{-2}$ (300–2500 K)

The enthalpy ΔH_T, entropy ΔS_T, and heat capacity ΔC_p of each species considered were calculated using the following relations:

$$\Delta H_T = \Delta H_{298.15} + \int_{298.15}^{T} \Delta C_p \, dT + \sum \Delta H_{\mathrm{tr}} \tag{4}$$

$$\Delta S_T = \Delta S_{T_1} + \int_{T_1}^{T} \frac{\Delta C_p}{T} dT + \sum \frac{\Delta H_{\mathrm{tr}}}{T_{\mathrm{tr}}} \tag{5}$$

$$C_p = A + B10^{-3}T + C10^{5}T^{-2}. \tag{6}$$

In these equations ΔH_{tr} and T_{tr} represent, respectively, the enthalpy and temperature associated with any phase transition encountered between the reference temperature (298.15 K) and the temperature of interest.

The free energy ΔG_T for each species considered was then calculated using the relation

$$\Delta G_T = \Delta H_T - T\Delta S_T, \tag{7}$$

T being the Kelvin temperature at which reaction (1) takes place. The equilibrium constant K_p is thus evaluated from

$$\ln K_p = \frac{-\Delta G}{RT}. \tag{8}$$

For the reaction

$$\mathrm{Zn_{(l)}} \rightleftarrows \mathrm{Zn_{(g)}}, \tag{9}$$

the heat of vaporization of zinc is calculated by equation (3) as

$$\left(\frac{\partial\left(\Delta H_{\mathrm{Zn}}\right)}{\partial T}\right)_P = C_{p(\mathrm{g})} - C_{p(\mathrm{l})} = -10.60. \tag{10}$$

After integration, equation (10) becomes

$$\Delta H_{\mathrm{Zn}} = \Delta H_0 - 10.60\,T. \tag{11}$$

where ΔH_0 is the integration constant.

The calculation of ΔH_0 is made by the Clapeyron-Clausius equation

$$\frac{\partial p}{\partial T} = \frac{\Delta H}{T\Delta V}. \tag{12}$$

The molar volume V_{l} of the condensed phase will be small and can be neglected in comparison with V_{g} the molar volume of the vapor; equation (12) will then become

$$\frac{\partial p}{\partial T} = \frac{\Delta H}{TV_g}. \tag{13}$$

The vapor pressure is relatively small and the vapor may be supposed to obey the ideal gas laws, so that $V_{\mathrm{g}} = \frac{RT}{p}$; substituting this into equation (13) gives us

$$\frac{\partial \ln p}{\partial T} = \frac{\Delta H}{RT^2}. \tag{14}$$

Putting ΔH_{Zn} into equation (14) gives us the result

$$\int_{p_1}^{p_2} R\, d(\ln p) = \int_{T_1}^{T_2} \left(\frac{\Delta H_0 - 10.60\, T}{T^2} \right) dT. \tag{15}$$

Upon performing the indicated integration, we have the result

$$R \ln \left(\frac{p_2}{p_1} \right) + 10.60 \ln \left(\frac{T_2}{T_1} \right) = \Delta H_0 \left(\frac{T_2 - T_1}{T_1 T_2} \right). \tag{16}$$

Substituting $\frac{p_2}{p_1} = \frac{m_2 T_2}{m_1 T_1}$, into equation (16), it is possible to calculate ΔH_0 if the mass at two temperatures are known.

Keeping the ZnO powder for ten minutes in hydrogen atmosphere at temperatures 1000 K, 1043 K and 1100 K, causes the mass to decrease as follows:

$$\begin{array}{rcl} m_{(1000\mathrm{K})} & = & 0.0684 \text{ g}, \\ m_{(1043\mathrm{K})} & = & 0.119 \text{ g, and} \\ m_{(1100\mathrm{K})} & = & 0.223 \text{ g}. \end{array} \tag{17}$$

On substitution of these values into equation (16), we find $\Delta H_0 = 128260\ \mathrm{J} \cdot \mathrm{mol}^{-1}$, and the heat of vaporization of zinc is

$$\Delta H_{\mathrm{Zn(g)}} = 128260 - 10.6\, T$$

The variation of the change in enthalpy of the complete reaction (1) at the temperature is then given by

$$\Delta H_T = 1.175 \times 10^{-3}\, T^2 - 25.49\, T + 2\,46220 - \frac{8.96 \times 10^5}{T}. \tag{18}$$

The calculation of the change in entropy of one mole of zinc vapor must be done according to the reversible cycle, which is composed of the following stages:

1. heating of zinc until the melting point;
2. fusion at the temperature 692.7 K;
3. heating of melted zinc until the temperature 1181 K;
4. evaporation of zinc at the boiling point;
5. cooling of gas atomic zinc until the temperature of interest.

The entropy change of the zinc will then be given by

$$\Delta S_{\mathrm{Zn(g)}} = S^0_{298.15} + \int_{298.15}^{T_f} \frac{C_{P(\mathrm{c})}}{T} dT + \frac{H_{\mathrm{l} \rightleftarrows \mathrm{c}}}{T_f} + \int_{T_f}^{T_b} \frac{C_{P(\mathrm{l})}}{T} dT + \frac{H_{\mathrm{g} \rightleftarrows \mathrm{l}}}{T_b} + \int_{T_b}^{T} \frac{C_{P(\mathrm{g})}}{T} dT\ .$$

Upon performing the indicated integration, we get

$$\Delta S_{\mathrm{Zn(g)}} = 42.762 + 20.82 \ln T.$$

The variation of the change in entropy of the complete reaction (1) at the temperature is then given by

$$\Delta S_T = 2.35 \times 10^{-3} T + 325.84 - 25.52 \ln T - \frac{4.48 \times 10^5}{T^2}. \tag{19}$$

The variation of the change in the free energy of the reaction (1) at the temperature is

$$\Delta G_T = -1.175 \times 10^{-3}\, T^2 - 351.33\, T + 246220 - \frac{4.48 \times 10^5}{T} + 25.52\, T \ln T. \tag{20}$$

A large positive ΔG_T value shows the equilibrium position lies to the far left of the reaction (1) (products give reactants). Decreasing ΔG with increase in temperature indicates that the starting material ZnO will be transported from a zone of high temperatures towards a zone of lower temperatures.

The equilibrium constant for reaction (1) is

$$\ln K_p = 1.4133 \times 10^{-4} T - 3.0695 \ln T + 42.258 - \frac{29615}{T} + \frac{53885}{T^2} \tag{21}$$

Thus, knowledge of K_p allows prediction of the relative proportions of products and reactants in a reaction. Values computed from (20) and (21) for various temperatures are given in Table 2. The equilibrium constant for reaction (1) is small; it follows that in the equilibrium condition, the extent of the reverse reaction predominates over that of the forward reaction. The plot of $\log K_p$ against the reciprocal of the absolute temperature should be a straight line, at least as long as ΔH remains constant. The results for the equilibrium constant in the temperature range from 800 K to 1100 K are plotted in Figure 2; the slope of this line is equal to $-\Delta H/2.303R$. The enthalpy change accompanying reaction (1) is found to be 2.3 eV in the given range of temperature.

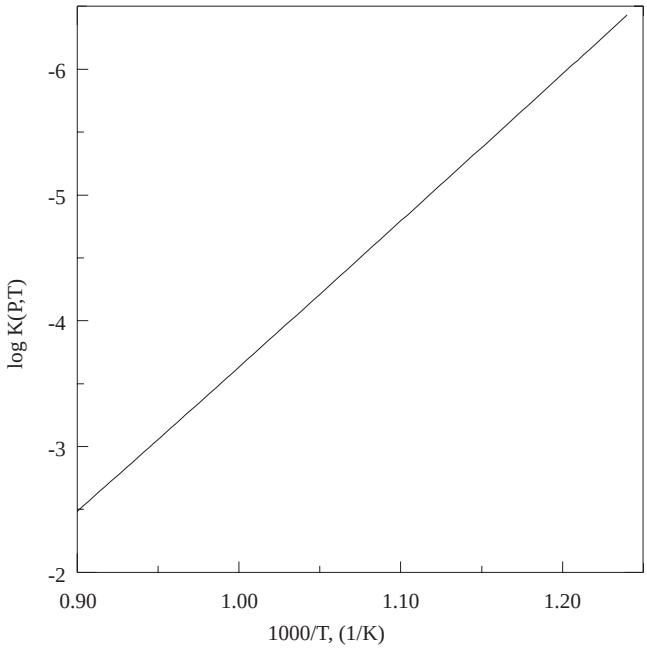

Figure 2. Plot of logarithm of equilibrium constant K_p of reaction (1) against the reciprocal of the absolute temperature ($\log K_p$ vs. T^{-1}).

3.2. Activation energy of reaction (1)

The activation energy of a reaction E_a is then defined as the additional energy which the reactant molecules must acquire in order to form the activated complex for the reaction. In other words, it is the difference in energy of the activated state and the reactants. The relationship between heat of reaction at constant pressure is given by equation

$$\Delta H = \Delta E + P\Delta V \tag{22}$$

Table 2. Computed values by ΔG_T and $\log K_p$ for different temperatures.

T (K)	ΔG_T $(\mathrm{J \cdot mol^{-1}})$	$\log K_p$
800	100320	-6.548
820	97195	-6.190
840	94083	-5.849
860	90982	-5.525
880	87891	-5.216
900	84811	-4.921
920	81740	-4.640
940	78679	-4.371
960	75628	-4.114
980	72586	-3.868
1000	69553	-3.632
1020	66529	-3.406
1040	63513	-3.189

where ΔV is the increase of volume when the reaction occurs at constant pressure P, and the change ΔE in the internal energy of the system must be exactly equivalent to the activation energy E_a of reaction (1). As will be evident shortly, E_a is an energy difference; it is the common practice, however, to omit the Δ symbol. If V is the volume of one mole of any gas, at the given temperature and pressure, then the total change of volume ΔV in the reaction will be equal to $V\Delta n$; equation (22) may therefore be written as

$$\Delta H = E_a + PV\Delta n.$$

In this case, Δn is 1, and the gases are assumed to behave ideally, PV is equal to RT and hence

$$\Delta H = E_a + RT. \tag{23}$$

For an endothermic reaction, for which ΔH is positive, the activation energy of the reaction E_a must be at least equal to the change ΔH in the enthalpy for the complete reaction. The activation energy of reaction (1) calculated from the equation (23) is 2.2 eV.

3.3. Fraction of the zinc present in the gaseous phase

The molar fraction of each constituent present at equilibrium are given by:

H_2	Zn	H_2O
$1-\alpha$	α	α

where α is the mole fraction of Zn present in the gaseous phase. The total number of moles present at equilibrium is $1+\alpha$. The total pressure is P, and the partial pressures are:

$$p_{H_2} = P\frac{1-\alpha}{1+\alpha}; \qquad p_{H_2O} = P\frac{\alpha}{1+\alpha}; \qquad p_{Zn} = P\frac{\alpha}{1+\alpha}\ . \tag{24}$$

The equilibrium constant K_p in terms of partial pressures for the reaction (1) is given by

$$K_p = \frac{p_{H_2O}p_{Zn}}{p_{H_2}}. \tag{25}$$

Introducing (24) into equation (25) the expression for the equilibrium constant becomes

$$K_p = P\frac{\alpha^2}{1-\alpha^2}. \tag{26}$$

It is evident from this result that if K_p is known, the molar fraction of the zinc vapor at equilibrium can be readily calculated at any pressure.

The variation of α with pressure may be derived by solving equation (26); thus,

$$\alpha = \sqrt{\frac{K_p}{P + K_p}}. \tag{27}$$

It is obvious from these result that the mole fraction of zinc present in the gaseous phase must decrease with increasing pressure. The calculations using equation (27) show that already at temperatures ranging between 800 and 880 K, for the reaction (1), we have practically a passage of the zinc atoms in the gaseous phase (Figure 3).

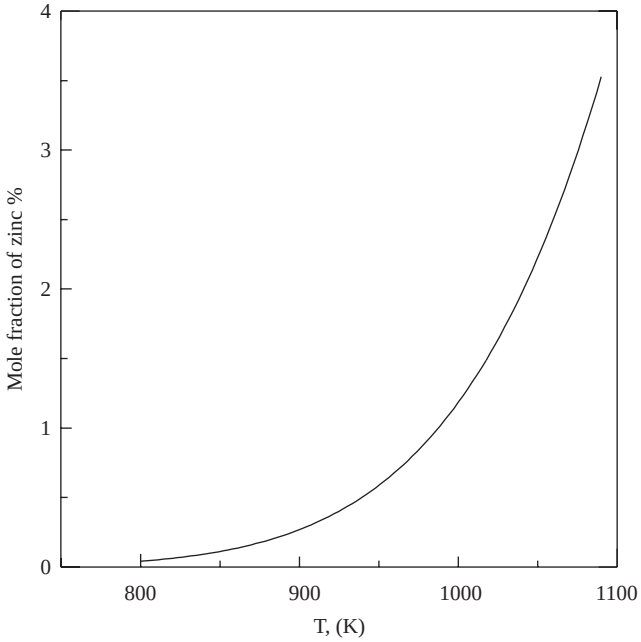

Figure 3. Variation of molar fraction α of zinc present in gaseous phase with temperature.

With respect to reaction (1), this particular relation of the parameters, including total pressure, allows Zn thin film depositions on substrates at temperatures ranging between 680 K and 1020 K. Experiments show that the reaction evolves at a substantial speed at the substrate temperature of 880 K.

3.4. Growth regimes

In our experiments, a total pressure of 0.166 MPa and $\Delta T = T_{crucible} - T_{substrate} = 120$ K, were maintained at constant levels. Generally, the growth rate G of the film can be described as

$$G = G_0 \exp\left(-\frac{E}{RT}\right) \tag{28}$$

where G_0, E, R and T are the preexponential factor, apparent activation energy, gas constant, and absolute temperature, respectively.

In Figure 4, we can see in a logarithmic plot the growth rate as a function of the inverse substrate temperature. Two growth temperature regions are present. For low temperatures (below 880 K), the film growth rate increases exponentially with substrate temperature according to an Arrhenius behavior, in which the deposition rate is controlled by an activated process such as adsorption, surface chemical diffusion,

chemical reaction and desorption. The growth rate is thus controlled by mass transfer and reaction kinetics. For the ZnO thin films deposition in this region, the activation energy of the growth rate determined from a least-square fit for the Arrhenius plot is 2.1 eV. This result is in good agreement with a previous theoretical calculation ($E_a = 2.2$ eV). At temperature above 880 K, the growth rate reaches its maximum and remains constant, indicating that the growth rate is diffusion limited. The growth rate strongly depends upon the substrate temperature.

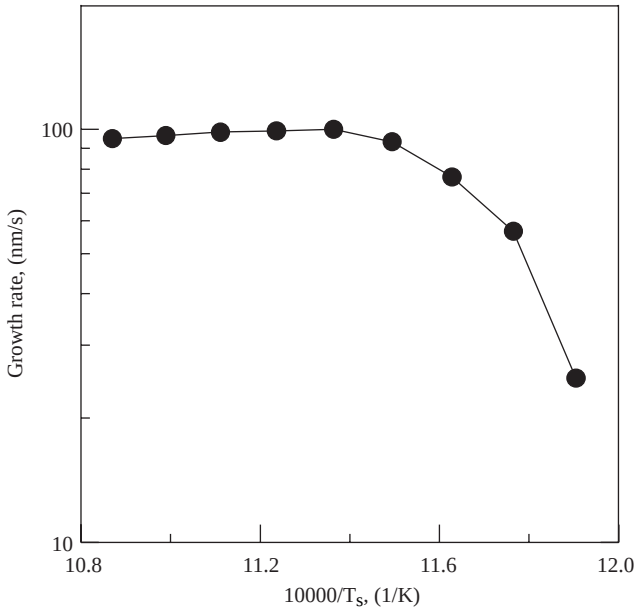

Figure 4. Evolution of the growth rate vs. inverse of substrate temperature T_s.

3.5. Green luminescence study of ZnO single-crystal thin films

A broad visible band is observed in our experiment, and is very similar to the early results reported by [35, 43, 45]. We have maintained ZnO samples in hydrogen atmosphere at various temperatures. These samples have been annealed at 1200 K in air for at least 2 h. Such annealing has allowed us to remove the individual properties of original samples. The stationary excitation of ZnO thin films, obtained via reaction (1), by a Xe arc lamp gives a PL with a large structureless spectral band that ranges from 440 nm to 680 nm with a radiation maximum centered on $\lambda = 510$ nm ($E = 2.42$ eV) with a full width at half maximum (FWHM) of 400 meV. ZnO films obtained at 800 K substrate temperature and at a growth rate of $6\mu\text{m}\cdot\text{min}^{-1}$ generate the most intense green luminescence. Thus, we are able to control the degree of influence of hydrogen on the annealing of ZnO for this wavelength (510 nm). Figure 5 shows a typical PL spectra of ZnO single-crystal thin films grown on sapphire measured at room temperature. Figure 6 shows the variation of the green luminescence intensities of ZnO ($\lambda = 510$ nm) measured at room temperature according to the conditions of the subsequent processing in a hydrogen atmosphere. The experiment shows that a reduction of green luminescence intensity of ZnO is possible upon keeping the ZnO in a hydrogen atmosphere at a temperature of 605 K. With a subsequent increase in the annealing temperature, the intensity of the green luminescence decreases, and is minimal at 820 K. According to these results, we can assert that, in the temperature range between 605 K and 820 K, conditions of the following reactions are verified:

$$\left| \begin{array}{lcll} \text{H}^+_{\text{chemisorbed}} & \rightarrow & (\text{O}-\text{H})^{2+} & + e^- \\ \text{H}^+_{\text{chemisorbed}} & \rightarrow & (V_{\text{O}}-\text{H})^{2+} & + e^- \end{array} \right\}. \tag{29}$$

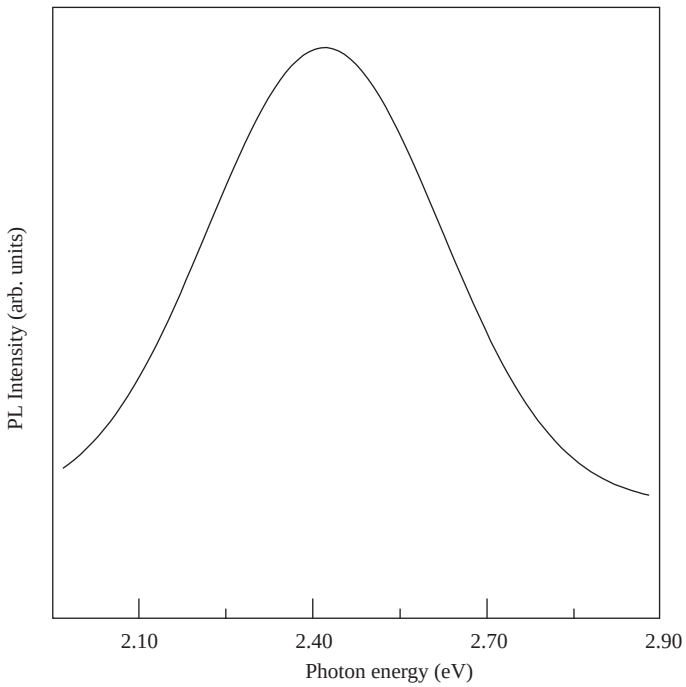

Figure 5. Photoluminescence spectrum of ZnO single-crystal thin films grown on sapphire measured at a room temperature.

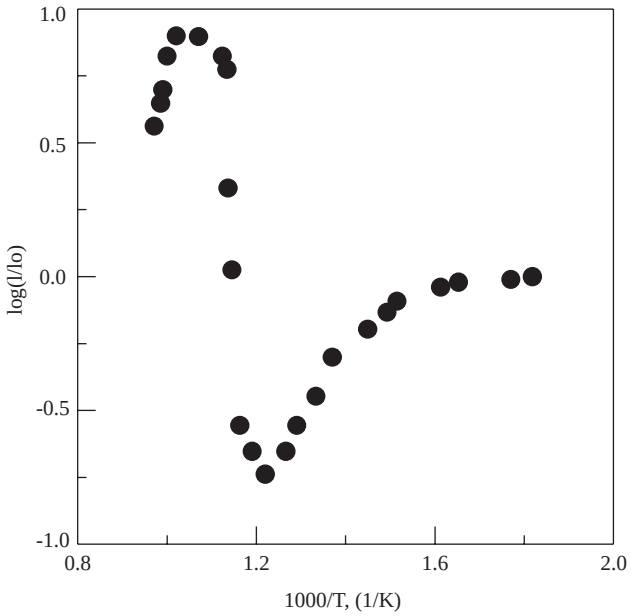

Figure 6. Logarithmic plot of the peak intensity of the green luminescence ($E = 2.42$ eV) in ZnO single crystal thin films against the inverse of temperature of hydrogen annealing. PL spectra measured at room temperature. I is the PL Intensity for ZnO after annealing in hydrogen atmosphere, and I_0 is the PL Intensity for ZnO without annealing in hydrogen atmosphere.

The first stage of the hydrogen interaction with ZnO begins with its chemisorption and dissociation according to the reaction:

$$\frac{1}{2}\mathrm{H}_2 \rightleftarrows \mathrm{H}^+_{\mathrm{chemisorbed}} + e^-. \tag{30}$$

At a relatively low temperature (300 K), hydrogen with a superficial atom is absorbed by atoms of oxygen present at the surface of the ZnO, as well as by atoms of zinc, according to the reaction

$$\mathrm{ZnO} + \mathrm{H}_2 \rightarrow \mathrm{ZnH} + \mathrm{OH}. \tag{31}$$

Defect complexes and/or residual impurities should be examined to account for the effects of native donors in ZnO [40]. FTIR (Fourier Transform Infrared) experiments with hydrogen on ZnO surfaces are usually made on powders. Two main absorption peaks have been assigned to dissociatively absorbed H_2: the first is the O-H vibration peak at 3510 cm^{-1} and the second is the Zn-H peak at 1710cm^{-1} [42]. With increase of sample temperature to 370 K, the binding energy of ZnH $\simeq$ 0.21 eV, the ZnH group becomes improbable to exist according to thermodynamics. The concentration of OH bonds increases slowly with temperature, since their energy (0.44 eV) is twice that of the ZnH bonds. Beyond 580 K, the predominant process becomes the diffusion of chemisorbed hydrogen in ZnO. At this stage, reactions involving the interaction of hydrogen with ZnO (25) are verified. Complexes of the type $(V_O - \mathrm{H})$ in ZnO are without luminescence. When compared to the original samples, $(V_O - \mathrm{H})$ provokes a five-fold drop off in the relative intensity of the green luminescence samples maintained in hydrogen at 820 K. The experiment shows also that subsequent samples annealing carried out in air and under vacuum conditions does not allow re-establishing their original luminescence. Therefore, we can consider that the dissolution of hydrogen in the ZnO is an irreversible process.

A model for the kinetics of the radiative and non-radiative processes in nanocrystalline ZnO particles has been proposed by van Dijken et al. [41], based on the assignment of the visible emission to a recombination of a shallowly trapped electron with a deeply trapped hole. From the particle size dependence of the emission properties, it is concluded that the photogenerated hole is trapped in a surface system (probably $\mathrm{O}^{2-}/\mathrm{O}^-$). The surface-trapped hole can tunnel back into the particle where it recombines with an electron in an oxygen vacancy (V_{O}^+) resulting in the creation of a V_{O}^{2+} center, the recombination center for the visible emission. The probability dependence for this tunneling process on particle size is much larger than for nonradiative processes. This results in an increase of the visible emission intensity as the size of the ZnO particles decreases. The effect of hydrogenation on the luminescence property of ZnO crystal was investigated by means of cathodoluminescence [44]. It was found that hydrogen plasma treatment strongly passivates the green emission and enhances the band edge luminescence.

Beyond 820 K, the sensitive liberation of oxygen of the ZnO lattice begins with a formation of oxygen vacancies on the surface as well as in volume. This stage of hydrogen interacting process with ZnO can be expressed by the symbolic equation

$$\mathrm{H}_{2(g)} \rightarrow \mathrm{H_2O}_{(g)} + V_{\mathrm{O}}^{2+} + 2e^-. \tag{32}$$

Within the temperature range from 820 K to 980 K, reaction (32) is predominant, and the concentration of oxygen vacancies in the ZnO increases following an exponential law. The intensity of the green luminescence sample, which is annealed in hydrogen, increases according to a similar law. The intensity of the green luminescence sample annealed at 980 K is 43 times more intense than that of samples annealed at 820 K. Above 980 K, the predominant defects in ZnO become interstitial ions of zinc (Zn_i^+):

$$\mathrm{H}_{2(g)} + \mathrm{ZnO} \rightleftarrows \mathrm{H_2O}_{(g)} + \mathrm{Zn}_i^+ + e^-. \tag{33}$$

(A second interstitial ionization of the zinc is observed above 1000 K.)

Regarding the native donor, the electronic structure indicates that only the zinc interstitial or the zinc antisite can explain the n-type conductivity of undoped ZnO, whereas the oxygen vacancy with the lowest formation energy should be dominant under n-type conditions [43]. Beyond 870 K, this process continues intensively. The result of process (33) is that zinc ions and electrons begin to displace in the region of the boundary layer and linear defects of ZnO. The growth of metallic zinc germs goes with the coalescence of zinc ions in this region. During the experiment, a change in the color of the samples occurs. At the beginning of this process, it is gray-shaded. However, beyond 980 K it becomes dark. The observations of an exponential decrease in the luminescence intensity when the sample starts taking another color. This effect increases with the rise of the annealing temperature.

4. Conclusion

Thermochemical analysis show that, at temperatures between 800 K and 880 K, for reaction (1), we have, in practicality, passage of zinc atoms in the gaseous phase. The activation energy of the growth rate (2.1 eV) is in good agreement with a theoretical calculation (E_a=2.2 eV). The growth rate strongly depends upon the substrate temperature.

The luminescence intensity of ZnO depends strongly on the deposition and annealing temperature. In the sample deposited at substrate temperature varying from 850 K to 980 K, the singly ionized oxygen vacancies represent the predominant defects and are obtained by the reaction

$$2\mathrm{H}^{+}_{\mathrm{ZnO}} + 2e^{-} \rightleftarrows \mathrm{H_2O}_{(g)} + V^{+}_{\mathrm{O}} + e^{-}. \tag{34}$$

The present PL study allows us to propose a process of regulation of the F^{+} centers concentration in ZnO. The data allow us to choose technological conditions for films and crystal synthesis for manufacturing scintillators with a maximum of radiation intensity centered at $\lambda = 510$ nm.

References

[1] H. C. Pan, and B. W. Wessels, *Mater. Res. Soc. Symp. Proc.*, **152**, (1989), 215.

[2] J. Kioke, K. Shimoe, and H. Ieki, *Jpn. J. Appl. Phys.*, Part 1 **32**, (1993), 2337.

[3] M. Kadota, and C. Kondoh, *IEEE Trans. Ultrason. Ferroelectr. Freq. Control,* **44**, (1997), 658.

[4] U. Lampe, and J. Muller, *Sens. Actuators,* **18**, (1989), 269.

[5] D. M. Bagnall, Y. F. Chen, Z. Zhu, T. Yao, S. Koyama, M. Y. Shen and T. Goto, *Appl. Phys. Lett.*, **70***, (1997), 2230.*

[6] Y. Sato, and S. Sati, *Thin Solid Films,* **281**, (1996), 445.

[7] J. Muller, and S. Weissenrieder, *J. Anal. Chem. USSR,* **349**, (1994), 380.

[8] W.-C. Shih, and M.-S. Wu, *J. Cryst. Growth,* **137**, (1994), 319.

[9] S.A. Studenikin, Nickolay Golego, and Michael Cocivea, *J. Appl. Phys.*, **83**, N4, (1998), 2287.

[10] M. Dinescu, and P. Verardi, *Appl. Surf. Sci.*, **106**, (1996), 149.

[11] J. George, *Preparation of Thin Films*, (Marcel Dekker, Inc., New York- Basel-Hong Kong, 1990).

[12] A. Jimenez-Gonzalez, and R. Suarez-Parra, *J. Cryst. Growth*, **167**, (1996), 649.

[13] Y. Takahashi, M. Kanamori, A. Kondoh, H. Minoura, and Y. Ohya, *Jpn. J. Appl. Phys.*, Part 1, **33**(12A), (1994), 6611.

[14] M. Izaki, and T. Omi, *J. Electrochem. Soc.*, **144**, (1997), L3.

[15] Y. Natsume, H. Sakata, T. Hirayama, and H. Yanagida, *J. Appl. Phys.*, **72**, (1992), 4203.

[16] A. Hausmann, and B. Schallenberger, *Z. Phys. B*, **31**, (1978), 269.

[17] A. Pöppl, and G. Völkel, *Phys. Status Solidi A*, **121**, (1990), 195.

[18] V. A. Nikitenko, *Zh. Prikl. Spektrosk.*, **57**, (1992), 367.

[19] K. Vanheusden, C. H. Seager, W. L. Warren, D. R. Tallant, and J. A. Voigt, *Appl. Phys. Lett.*, **68**, (1996), 403.

[20] J. Zhong, A. H. Kitai, P. Mascher, and W. Puff, *J. Electrochem. Soc.*, **140**, (1993), 3644.

[21] N. Ohashi, T. Nakata, T. Sekiguchi, H. Hosono, M. Mizuguchi, T. Tsurumi, J. Tanaka, and H. Haneda, *Jpn. J. Appl. Phys.*, Part 2 **38**, (1999), L113.

[22] J. C. Simpson, and J. F. Cordaro, *J. Appl. Phys.*, **63**, (1988), 1781.

[23] R. A. Winston and J. F. Cordaro, *J. Appl. Phys.*, **68**, (1990), 6495.

[24] R. Krause-Rehberg, H. S. Leipner, T. Abgarjan, and A. Polity, *Appl. Phys. A*: Mater. Sci. Process., **66**, (1998), 599.

[25] R. M. de la Cruz, R. Pareja, R. Gonza´lez, L. A. Boatner, and Y. Chen, *Phys. Rev. B*, **45**, (1992), 6581.

[26] T. K. Gupta, W. D. Straub, M. S. Ramanachalam, J. P. Schaffer, and A. Rohatgi, *J. Appl. Phys.*, **66**, (1989), 6132.

[27] H. Wolf, S. Deubler, D. Forkel, H. Foettinger, M. Iwatschenko-borho, F. Meyer, M. Renn, W. Witthuhn, and R. Helbig, *Mater. Sci. Forum*, **10-12**, (1986), 863.

[28] S. Deubler, J. Meier, R. Schu¨tz, and W. Witthuhn, *Nucl. Instrum. Methods Phys. Res. B*, **63**, (1992), 223.

[29] P. H. Kasai, *Phys. Rev.*, **130**, (1963), 989.

[30] G. Muller, *Phys. Status solidi (b)*, **76**, (1976), 525.

[31] R. S. Soni, P. S. Divan, *J. Appl. Phys.*, **18**, (1980), 292.

[32] F. A. Kroger and H. J. Vink, *J. Chem. Phys.*, **22**, (1954), 250.

[33] V. Soriano, D. Galland, *J. Status solidi (b)*, **2**, (1976), 739.

[34] W. F. Wei, *Phys. Rev. B.*, **15** , (1977), 2250.

[35] K. Vanheusden, W. L. Warren, C. H. Seager, D. R. Tallant, J. A. Voigt, and B. E. Gnade, *J. Appl. Phys.*, **79**, (1996), 7983.

[36] K. Vanheusden, C.H. Seager, W.L. Warren, D.R. Tallant, J. Caruso, M. J. Hampden-Smith, and T. T. Kodas, *J. Lumin.*, **75**, (1997), 11.

[37] Handbook of chemistry and physics 66th edition, Editor-in-Cheif Robert C Weast CRC press Inc. Boca Raton Florida U.S.A (1986).

[38] Handbook of thermodynamic Data, G. B. Naumov, B. N. Ruzkenko, and I. L. Khodakovsky, original published by the USSR Academy of Sciences Atomizdat. PB226-722+328pp (1971).

[39] Perry's Chemical Engineers Handbook seventh edition Robert H Perry, Don W Green, Mc Graw-Hill international editions (1998).

[40] G. D. Mahan, *J. Appl. Phys.*, **54**, (1983), 3825.

[41] A. van Dijken, E.A. Meulenkamp, D. Vanmaekelbergh, A. Meijerink, *J. Lumin*, **87-89**, (2000), 454.

[42] G. Ghiotti, A. Chiorino, F. Bocuzzi, *Surf. Sci.*, **287**, (1993), 228.

[43] Fumiyasu Oba, Shigeto R. Nishitani, Seiji Isotani, Isao Tanaka and Hirohiko Adachi, *J. Appl. Phys.*, **90**, (2001), 824.

[44] Takashi Sekiguchi, Naoki Ohashi and Yoshihiro Terada, *Jpn. J. Appl. Phys.*, Part 2, **36**, (1997), L289.

[45] Zhang W. L. et al., *Chin. Phys. Lett.*, **16,** (1999), 728.